PAPER • OPEN ACCESS

Improved geometric and recollision estimates for the invariance principle of the random Lorentz gas

To cite this article: Karsten Matthies and Raphael Winter 2026 *Nonlinearity* **39** 035003

View the article online for updates and enhancements.

Check for updates

PAPER

Improved geometric and recollision estimates for the invariance principle of the random Lorentz gas

Karsten Matthies[1] and Raphael Winter[2,*]

[1] Department of Mathematical Sciences, University of Bath, Bath, United Kingdom
[2] School of Mathematics, Cardiff University, Cardiff, United Kingdom
[*] Author to whom any correspondence should be addressed.

E-mail: winterr6@cardiff.ac.uk and k.matthies@bath.ac.uk

Abstract

By improving geometric recollision estimates for a random Lorentz gas, we extend the timescale $T(r)$ of the invariance principle for a Lorentz gas with particle size r obtained by Lutsko and Tóth (2020) from $\lim_{r\to 0} T(r) r^2 |\log(r)|^2 = 0$ to $\lim_{r\to 0} T(r) r^2 |\log(r)| = 0$. We show that this is the maximal reachable timescale with the coupling of stochastic processes introduced in the original result. In our improved geometric estimates we make use of the convexity of scatterers to obtain better dispersive estimates for the associated billiard map. We provide additional estimates on the exit distribution of simple recollisions.

1. Introduction

The dynamical behaviour of a hard-sphere flow between fixed scatterers is a classical topic in the theory of billiards as well as in mathematical statistical physics for the emergence of diffusion. In this paper, we use billiard maps to extend the time scales for which diffusive behaviour can be established.

We consider the random Lorentz gas in $\mathbb{R}^3$, i.e. balls of radius r, infinite mass and with centres distributed by a Poisson point process of intensity ρ such that $r^2 \rho$ is bounded. We are interested in the trajectory $t \mapsto X^{r,\rho}(t) \in \mathbb{R}^3$ of a point particle starting at the origin in a random unit direction, with free flights between collisions and elastic collisions with the scatterers. For fixed times $t \in [0, T]$, the process $t \mapsto X^{r,\rho}(t)$ converges in a Boltzmann–Grad scaling ($r \to 0$, $\rho \to \infty$ and $r^2 \rho \to 1$) to a Markovian flight process $X(t)$ and the distribution can be described by kinetic equations as shown originally by Gallavotti [10], Spohn [29] and Boldrighini–Bunimovich–Sinai [6]. For more recent results, see Golse [11] and references therein. The main difference between the random Lorentz gas and a random flight process is that the latter is independent of its past, so it ignores the positions of previous scatterers and it allows collisions at places where in the past had not been any scatterers (*shadowed scattering*). Additionally, the point particle in a Lorentz gas can have *recollisions* with previous scatterers. These are the two main effects that need to be controlled in convergence proofs.

Diffusive behaviour can be observed for the free-flight process after a further rescaling

$$t \mapsto \frac{X(Tt)}{\sqrt{T}} \quad \text{for } T \to \infty, \tag{1.1}$$

such that even better control of shadowed scattering and recollisions is necessary when this is to be extended to the Lorentz gas. Lutsko and Tóth [13] prove an invariance principle (i.e. diffusive behaviour in the scaling of (1.1)) in a combined Boltzmann–Grad and diffusive limit $r \to 0$, $\rho \to \infty$, $r^2 \rho \to 1$ and $T(r) \to \infty$, such that $\lim_{r\to 0} T(r) r^2 |\log(r)|^2 = 0$. The convergence holds when averaging over the random initial velocity and random placement of scatterers. The key technical innovation is to use probabilistic

coupling arguments involving three processes: the Lorentz gas X, the Markovian flight process Y and an auxiliary process Z that has some memory, but only until the previous collision event. Lutsko and Tóth combine the probabilistic arguments with an analysis of the three dimensional geometry of the tracer particle bouncing between two scatterers of the same size.

In this paper, we give improved estimates by analysing a billiard map on the two scatterers and we extend the time-scale of the combined Boltzmann–Grad and diffusive limit to $T(r) \to \infty$ under the condition $\lim_{r\to 0} T(r)r^2|\log(r)| = 0$. We note that Lutsko and Tóth achieved such an improved time-scale in the simpler geometry of the wind-tree process [14]. In our analysis of the Lorentz gas, a separation of the two cases, where the distance between the scatterers is smaller or larger than a fixed multiple of their radius, is advantageous. Several effects that are estimated to be of order $r^2|\log(r)|^2$ in [13] will be shown to be of order r^2. We do not re-analyse other effects that lead to errors of $r^2|\log(r)|$. This immediately allows us to use the same methods as in [13] as well as gaining further insights about the dynamic behaviour. In particular, we also show that after a simple recollision the exit velocity distribution regains independence of the initial velocity and is $\mathrm{Uni}(\mathbb{S}^2)$ distributed in the critical case when the distance between the scatterers is large, see lemma 2.7.

We stress the fact that the result presented here realises the maximal timescale attainable with bounds on direct shadowing/recollision events. More precisely, the coupling of the Z-process and the Lorentz gas process X fails beyond the timescales determined by $\lim_{r\to 0} T(r)r^2|\log(r)| = 0$. This follows from the observation that mechanical inconsistencies after two collisions (i.e. indirect recollisions) appear beyond this timescale and are not respected by the Z-process, see remark 3.3. The same holds for inconsistencies between two subsequent flights in the presence of a direct shadowing event. An interesting question for future research is whether a more elaborate auxiliary process, possibly one having memory of the last two scatterers, would allow us to extend the results to times $T(t)$ under the condition $\lim_{r\to 0} T(r)r^2 = 0$. This likely requires significant technical effort. Finally, we recall that on timescales $T(r) \sim r^{-2}$ complex recollision patterns of arbitrary length seem to be present that likely require entirely new tools, see also [13, remarks on dimension (3)(b)].

Related work: The statistical and long-term diffusive behaviour has been analysed for various models related to the random Lorentz gas. Tóth recently showed the invariance principle for almost all realisations just suitably averaging over initial velocities [31]. Lutsko and Tóth adapted their ideas to the wind-tree process [14] and to Lorentz gases with an underlying magnetic field [15] using earlier work on the magnetic Lorentz gas by Nota, Saffirio and Simonella [24]. Nota, Nowak and Saffirio also analyse the magnetic case in [23]. Different scaling behaviour for the Lorentz gas can be observed for periodically placed scatterers, see the works by Caglioti-Golse [7] and Marklof–Strömbergsson [16–18]. In this case, a kinetic description by linear Boltzmann equations is not possible and for longer times a superdiffusive behaviour can be observed [19] as well as a non-standard central limit theorem [1]. However, Wennberg was able to derive a linear Boltzmann equation for a Lorentz Gas with nearly periodic scatterer distribution, see [32]. Diffusive behaviour has also been shown for a particle in a suitable random forcefield on $\mathbb{R}^d$ for $d \geqslant 3$ in [8] and on $\mathbb{R}^2$ in [12].

In an idealised Rayleigh gas the background particles are of finite mass and move, but do not interact with each other. In the kinetic limit, a linear Boltzmann equation can be derived [30] for hard-sphere interactions, for a general conservative situation see [20] and with annihilation [27]. In the conservative setting, if the background particles are Maxwell-distributed, diffusive behaviour can be observed on time-scales below $r^{-1/8}$, see [21]. Fractional diffusion can be derived for suitable short-range interactions between the tagged particle and background particles with a fat-tailed distributions for time-scales below $r^{-\alpha}$ for some small $\alpha > 0$, see [22].

In a non-idealised Rayleigh gas, the background particles interact with each other, but are assumed to be in equilibrium. In this considerably more complex system, diffusive behaviour has been shown in [2] for a double logarithmic timescale, which has recently been improved to $(\log|c_\beta \log r|)^{1/2-\alpha}$ in [9]. More general fluctuations around the equilibrium in the full hard sphere flow lead to fluctuating Boltzmann equations, see the recent woks by Bodineau, Gallagher, Saint-Raymond, and Simonella [3–5]. For more details on scaling limits of tagged particles in random fields, see [25, 26].

Plan of paper: We introduce the setup for direct recollisions in the next section. The main improved geometric estimate is given in section 2.1, this will yield a better control of the probability of scattering events in section 2.2. Additional independence results are shown in section 2.3. The results are applied to the invariance principle in section 3 by sketching the relevant improvements of [13].
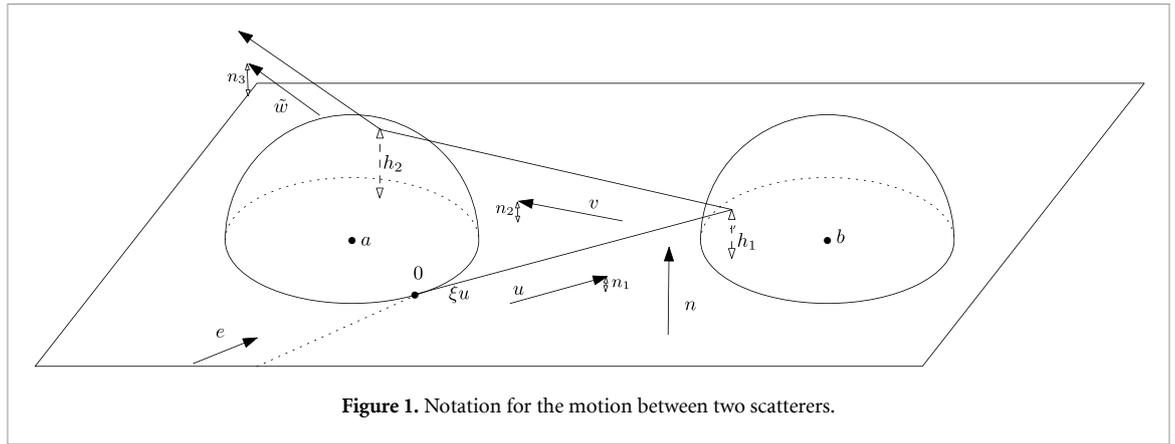
Figure 1. Notation for the motion between two scatterers.

2. Recollisions of the tracer particle with two scatterers

In this section, we present the geometric improvements on the probability of collision events. In order to keep the presentation self-contained, we review the main elements of the geometric argument introduced in [13]. We use variables $(u,\xi,v) \in \mathbb{D} = \mathbb{S}^2 \times \mathbb{R}^+ \times \mathbb{S}^2$ to parametrise possible direct recollisions, i.e. backscattering of the tracer particle to an obstacle after the subsequent collision. Without loss of generality we fix the incoming velocity for the first collision to be the first unit vector $e = e_1 \in \mathbb{R}^3$. In the set of variables $(u,\xi,v) \in \mathbb{D} = \mathbb{S}^2 \times \mathbb{R}^+ \times \mathbb{S}^2$, the velocity u then represents the velocity after the first collision, v the velocity after the second collision, and ξ the free flight time in between. Throughout this section we use the geometric notation as summarised in figure 1.

Definition 2.1 (Recollision events). Given a radius $r > 0$, a recollision event is determined by $(u,\xi,v) \in \mathbb{D}$, where $\mathbb{D} = \mathbb{S}^2 \times \mathbb{R}^+ \times \mathbb{S}^2$. For $(u,\xi,v) \in \mathbb{D}$, we define the process $\tilde{Z}_r(t) \in \mathbb{R}^3$, $t \in \mathbb{R}$ by

1. $\tilde{Z}_r(0) = 0$, and $\tilde{Z}_r(t) = te$ for all $t < 0$, where $e = e_1$ is the first coordinate vector.
2. $\tilde{Z}_r(t) = tu$, for $t \in (0,\xi)$.
3. The centres $a,b \in \mathbb{R}^3$ of the two obstacles are defined by

$$a := r\frac{e-u}{|e-u|}, \quad b := \xi u + r\frac{u-v}{|u-v|}. \tag{2.1}$$

4. $\tilde{Z}_r(t)$ for $t \geqslant \xi$ given by dynamics of a point particle interacting with the infinite mass hard-sphere obstacles $B_r(a)$ and $B_r(b)$ with $\dot{\tilde{Z}}_r(\xi^+) = v$.
5. Let N be the total number of collisions of this process, and denote by w_k, $0 \leqslant k \leqslant N$ the velocity after the kth collision with $w_0 = e$, $w_1 = u$, $w_2 = v$. Similarly, define $0 = \tau_1 \leqslant \tau_1 \leqslant \cdots \leqslant \tau_N$ as the collision times of the process.
6. We denote by $\tilde{\beta}$ the time of the last collision and $\tilde{w} = w_N$ the outgoing velocity.

By rescaling, we will later reduce the analysis to the case $r = 1$, so we introduce the short-hand $\tilde{Z} = \tilde{Z}_1$.

Notice that the position of the second scatterer is determined by $(u,\xi,v) \in \mathbb{D}$ and $r > 0$, and we do not exclude the possibility of overlap between the scatterers. In the next lemma, we summarise the geometric arguments used in [13] to estimate the probability of specific recollision events.

Lemma 2.2. [13, Section 6.5.3] *Let $r = 1$ and $(u,\xi,v) \in \mathbb{D}$. Define $n \in \mathbb{S}^2$ to be a unit vector perpendicular to the plane generated by the points $0,a,b$, more precisely*

$$n := \frac{a \times b}{|a||b|\sin(\angle(a,b))}, \tag{2.2}$$

and $n_k := w_k \cdot n$ the velocity component along this direction. Then the following holds:

1. n_k *is monotone increasing if $n_1 \geqslant 0$, i.e. $n_k \geqslant n_{k-1}$ for $1 \leqslant k \leqslant N$.*
2. *We have the following bounds for the trapping time and angles*

$$\tilde{\beta} \leqslant \xi + |w_1|^{-1}, \tag{2.3}$$

$$\angle\left(-e, w_j\right) > \frac{\pi}{2} - \angle\left(n, w_j\right), \tag{2.4}$$

$$|n_2| = |v \cdot n| \geqslant \tfrac{1}{2}|e \cdot (u \times v)|. \tag{2.5}$$

3. *If u, v are i.i.d.* $\mathrm{Uni}(\mathbb{S}^2)$ *distributed, then* $w := \frac{u \times v}{|u \times v|}$ *and* $\vartheta := |u \times v|$ *are independent and w is again* $\mathrm{Uni}(\mathbb{S}^2)$ *distributed, while* $\vartheta \sim \mathbb{1}_{[0,1]} \frac{t}{\sqrt{1-t^2}} dt$.

2.1. Improved geometric estimates

The approach in this contribution is based on making quantitative improvements on the estimates in [13]. In lemma 2.3, we give improved estimates for the probability of certain recollision events depending on the total number of collisions N and the free flight time ξ after the first collision. Rescaling allows us to restrict, without loss of generality, to the case $r = 1$.

For recollisions with short free flight times, meaning $\xi > 0$ small, the two scatterers can be close, touch, or even overlap. For such events, we will use the bounds introduced in [13] and reviewed above. On the other hand, for $\xi \to \infty$ we introduce the new estimates that allow us to eliminate the logarithmic divergence in the resulting estimate. Hence, we now restrict our attention to large flight times $\xi \geqslant 10$, where the value 10 is chosen for convenience.

We also remark that the estimate by Lutsko and Tóth is sharp when $N = 3$ is the total number of collisions introduced in definition 2.1. Therefore, we will primarily consider the case $\xi \geqslant 10$ and $N \geqslant 4$. Here the convexity of the spheres leads to improved estimates on the components n_i allowing for sharper estimates on the trapping time. The estimates are closely related to the dispersive properties of Sinai-billiards introduced in [28]. The following lemma encodes the main gain in the scattering estimates due to the convexity of the obstacles. We provide quantitative estimates for the increase for the n_k depending on height above the plane of the scatterers as described in the basic geometric set-up in figure 1.

Lemma 2.3. *Let $(u, \xi, v) \in \mathbb{D}$ be such that the total number of collisions satisfies $N \geqslant 3$, and further assume $\xi \geqslant 10$, and $n_1 \geqslant 0$. Recall the definition of n in (2.2) and let $h_i := \tilde{Z}(\tau_i) \cdot n$, where $0 = \tau_1 \leqslant \tau_1 \leqslant \cdots \leqslant \tau_N$ are the collision times. Then the following inequalities hold*

$$\begin{cases} h_{k+1} & \geqslant h_k + \frac{1}{2}\xi\, n_{k+1}, \\ n_{k+1} & \geqslant n_k + h_k, \end{cases} \quad \text{for } 1 \leqslant k \leqslant N-1. \tag{2.6}$$

Proof. For the first inequality, we first observe $n_1 \geqslant 0$ and n_k monotone increasing implies by using $h_{k+1} = h_k + (\tau_{k+1} - \tau_k)n_{k+1}$ for $k \geqslant 1$ that $h_k \geqslant 0$ is increasing as well. Since $\xi \geqslant 10$, the free flight time is bounded below by

$$\tau_{k+1} - \tau_k \geqslant \frac{1}{2}\xi, \tag{2.7}$$

which implies the first inequality (notice that this lower bound does not hold for ξ approaching zero).

For the second inequality we use that the flights $F_{k+1} = (\tau_{k+1} - \tau_k)w_{k+1}$ and $F_k = (\tau_k - \tau_{k-1})w_k$ need to satisfy

$$|F_{k+1} + F_k| \leqslant 2,$$

to lead back to the same scatterer after two consecutive flights. Using the notation $T_k = \tau_k - \tau_{k-1}$ and $T_{k+1} = \tau_{k+1} - \tau_k$ as well as $T_k \wedge T_{k+1} = \min(T_k, T_{k+1})$ and $T_k \vee T_{k+1} = \max(T_k, T_{k+1})$, we write

$$|F_{k+1} + F_k| = |T_{k+1} \wedge T_k (w_{k+1} + w_k) + (T_k \vee T_{k+1} - T_k \wedge T_{k+1}) w_*|,$$

where w_* is the velocity corresponding to the larger of T_k, T_{k+1}. Since $|w_k| = |w_{k+1}|$, we have

$$(w_{k+1} + w_k) \cdot w_* \geqslant 0,$$

and from (2.7) we get $T_{k+1} \wedge T_k \geqslant 5$, so we obtain

$$5|w_{k+1} + w_k| \leqslant T_{k+1} \wedge T_k|w_{k+1} + w_k| \leqslant |F_{k+1} + F_k| \leqslant 2. \tag{2.8}$$

Let $V_k := \tilde{Z}(\tau_k) - c$, where $c \in \mathbb{R}^3$ is the centre of the scatterer hit in the kth collision. Then, by the elastic collision rule

$$w_{k+1} = w_k - 2(V_k \cdot w_k)V_k. \tag{2.9}$$

Together with (2.8) this yields

$$2\left|w_k - (V_k \cdot w_k)\, V_k\right| = |w_{k+1} + w_k| \leqslant \frac{2}{5},$$

which implies $V_k \cdot w_k \leqslant -\frac{4}{5}$. Here, we use that $V_k \cdot w_k \leqslant 0$ is necessarily negative, since a collision occurs. Inserting this inequality back into the n projection of (2.9) and noting that $h_k = V_k \cdot n$ gives

$$n_{k+1} \geqslant n_k + h_k,$$

and finishes the proof. □

2.2. Probability of scattering events

On the set $\mathbb{D}$ introduced in definition 2.1, we consider the measure

$$\mu = \mathrm{Uni}\left(\mathbb{S}^2\right) \times \mathrm{EXP}\left(1|1\right) \times \mathrm{Uni}\left(\mathbb{S}^2\right), \tag{2.10}$$

where $\mathrm{EXP}(1|1)$ is the unit exponential distribution on $\mathbb{R}^+$ conditioned to the interval $[0,1]$, i.e. the image measure on $[0,1]$ has the density

$$\rho_{1,1}\left(x\right) = \mathbb{1}_{[0,1]}\left(x\right) \frac{e^{1-x}}{e-1}.$$

A key point in [13] is played by the set of *shadowing events* $\hat{A}_r$, where the second scatterer is placed in the path of the tracer particle before hitting the first obstacle, and *recollision events* $\tilde{A}_r$, where the tracer particle scatters back to the first scatterer after hitting the second. They can be formally defined as

$$\hat{A}_r := \left\{ (u,\xi,v) \in \mathbb{D} : \inf\left\{ t : \left|\xi u + r\frac{u-v}{|u-v|} + te\right| < r \right\} < \infty \right\},$$

$$\tilde{A}_r := \left\{ (u,\xi,v) \in \mathbb{D} : \inf\left\{ t : \left|\xi u + r\frac{u-e}{|u-e|} + tv\right| < r \right\} < \infty \right\}.$$

We will also use the related set $\tilde{A}_r'$ given by

$$\tilde{A}_r \subset \tilde{A}_r' := \left\{ (u,\xi,v) \in \mathbb{D} : \angle(u,v) \leqslant 2r\xi^{-1} \right\}. \tag{2.11}$$

On the two sets respectively, we define $\hat{w}_r, \hat{\beta}_r$ and $\tilde{w}_r, \tilde{\beta}_r$ as

1. $\hat{w}_r := u,\ \hat{\beta}_r = 0$ (no trapping, second scatterer is ignored because of shadowing),
2. $\tilde{w}_r, \tilde{\beta}_r$ are given by the trajectory of the tracer particle bouncing between the two obstacles, where $\tilde{\beta}_r$ is the time of the last collision and $\tilde{w}_r$ the outgoing velocity.

We will improve the bounds on the likelihood of such events by estimating events with different numbers of collisions separately. Recall that for $r > 0$ and $(u,\xi,v) \in \tilde{A}_r$, we denote by $N = N(r,u,\xi,v)$ the number of collisions of the tracer particle between the two obstacles.

In the rest of this subsection, we will derive the following geometric bounds which improve the estimates in proposition 3 of [13]. We make use of a scaling argument to reduce to the geometric arguments to the case $r = 1$. In this case, we write $\tilde{A} = \tilde{A}_1$, $\tilde{w} = \tilde{w}_1$ and $\tilde{\beta} = \tilde{\beta}_1$ to simplify notation.

Lemma 2.4. *Let $r = 1$. Then for all $s > 0$ we have*

$$\lambda\left((u,\xi,v) \in \tilde{A} : \angle(-e,\tilde{w}) < s^{-1}, \xi \leqslant 10 \right) \leqslant \frac{C}{1+s}, \tag{2.12}$$

$$\lambda\left((u,\xi,v) \in \tilde{A} : \angle(-e,\tilde{w}) < s^{-1}, \xi \geqslant 10, N = 3 \right) \leqslant \frac{C}{1+s}, \tag{2.13}$$

$$\lambda\left((u,\xi,v) \in \tilde{A} : \angle(-e,\tilde{w}) < s^{-1}, \xi \geqslant 10, N \geqslant 4 \right) \leqslant \frac{C}{(1+s)^2}, \tag{2.14}$$

$$\lambda\left((u,\xi,v) \in \tilde{A} : \tilde{\beta} > s, N = 3 \right) \leqslant \frac{C}{1+s}, \tag{2.15}$$

$$\lambda\left((u,\xi,v) \in \tilde{A} : \tilde{\beta} > s, N \geqslant 4 \right) \leqslant \frac{C}{1+s^2}, \tag{2.16}$$

where the measure λ is given by

$$\lambda = \mathrm{Uni}\left(\mathbb{S}^2\right) \times \mathrm{Leb}\left(\mathbb{R}^+\right) \times \mathrm{Uni}\left(\mathbb{S}^2\right)$$

the uniform measure on $\mathbb{D}$.

As in [13], the lemma above can be used to obtain estimates for the probabilities of collision events with respect to the measure μ as defined in (2.10), by the same scaling argument outlined there.

Corollary 2.5. *The following improved geometric estimates hold*

$$\mu\left((u,\xi,v) \in \tilde{A}_r : \angle(-e,\tilde{w}_r) < s^{-1}, \xi \leqslant 10r\right) \leqslant \frac{Cr}{1+s}, \tag{2.17}$$

$$\mu\left((u,\xi,v) \in \tilde{A}_r : \angle(-e,\tilde{w}_r) < s^{-1}, \xi \geqslant 10r, N = 3\right) \leqslant \frac{Cr}{1+s}, \tag{2.18}$$

$$\mu\left((u,\xi,v) \in \tilde{A}_r : \angle(-e,\tilde{w}_r) < s^{-1}, \xi \geqslant 10r, N \geqslant 4\right) \leqslant \frac{Cr}{(1+s)^2}, \tag{2.19}$$

$$\mu\left((u,\xi,v) \in \tilde{A}_r : \tilde{\beta}_r > s, N = 3\right) \leqslant \frac{Cr}{1+s}, \tag{2.20}$$

$$\mu\left((u,\xi,v) \in \tilde{A}_r : \tilde{\beta}_r > s, N \geqslant 4\right) \leqslant \frac{Cr}{1+s^2}. \tag{2.21}$$

Remark 2.6. The corresponding estimates in proposition 3 of [13] feature an additional $|\log(s)|$ that the new estimates can avoid. The overall estimates involve integration with respect to s which introduces the single $|\log r|$ term remaining in our estimate.

Proof. [Proof of lemma 2.4] The proof of (2.12) is the same as in [13] (proof of (78) there), and the logarithm disappears since we restrict to $\xi \leqslant 10$.

To bound (2.13), we first observe that by (2.4)

$$\angle(-e,\tilde{w}) \geqslant \frac{\pi}{2} - \angle(w,n) \geqslant \frac{1}{2}n_3. \tag{2.22}$$

The latter can be bounded below using (2.6) and (2.5):

$$n_3 \geqslant n_2 + h_2 \geqslant \left(1 + \frac{1}{2}\xi\right)n_2 \geqslant \frac{1}{2}\left(1 + \frac{1}{2}\xi\right)|e \cdot (u \times v)|. \tag{2.23}$$

Inserting this into (2.22) allows us to estimate

$$\lambda\left((u,\xi,v) \in \tilde{A} : \angle(-e,\tilde{w}) < s^{-1}, \xi \geqslant 10, N = 3\right)$$
$$\leqslant \lambda\left((u,\xi,v) \in \tilde{A} : \tfrac{1}{2}n_3 \leqslant s^{-1}, \xi \geqslant 10, N = 3\right)$$
$$\leqslant \lambda\left((u,\xi,v) \in \tilde{A}' : \left(1 + \tfrac{1}{2}\xi\right)|e \cdot (u \times v)| \leqslant 4s^{-1}, \xi \geqslant 10, N = 3\right),$$

where in the last inequality we have also used the inclusion $\tilde{A} \subset \tilde{A}'$ in (2.11). We are now in the position to estimate the last line, by making use of the representation $u \times v = \vartheta w$ in part 3 of lemma 2.2. This reduces the claim to the integral bounds:

$$\lambda\left((u,\xi,v) \in \tilde{A} : \angle(-e,\tilde{w}) < s^{-1}, \xi \geqslant 10, N = 3\right)$$
$$\leqslant C \int_{10}^{\infty} \int_0^{1/\xi} \int_{\mathbb{S}^2} \mathbb{1}_{\frac{1}{2}\xi|e \cdot W| \leqslant 4/(st)} t \, \mathrm{d}S(W) \, \mathrm{d}t\mathrm{d}\xi$$
$$\leqslant C \int_{10}^{\infty} \int_0^{1/\xi} \frac{8t}{1 + 8s\xi t} \, \mathrm{d}t\mathrm{d}\xi \leqslant C \int_{10}^{\infty} \frac{1}{s\xi} \int_0^{1/\xi} \frac{8s\xi t}{1 + 8s\xi t} \, \mathrm{d}t\mathrm{d}\xi$$
$$\leqslant C \int_{10}^{\infty} \frac{1}{s\xi^2} \, \mathrm{d}\xi \leqslant \frac{C}{1+s}. \tag{2.24}$$

The estimate (2.14) follows analogously, using that for n_4 we have the stronger inequality

$$n_4 \geqslant h_3 \geqslant \tfrac{1}{2}\xi n_3 \geqslant \tfrac{1}{8}\xi^2|e \cdot (u \times v)|. \tag{2.25}$$

The main improvement of our method lies in estimating (2.15) and (2.16). First, we split into short and long recollisions:

$$\lambda\left((u,\xi,v)\in\tilde{A}:\tau>s\right)\leqslant\lambda\left((u,\xi,v)\in\tilde{A}:\tau>s,\xi\leqslant 10\right)+\lambda\left((u,\xi,v)\in\tilde{A}:\tau>s,\xi\geqslant 10\right).$$

The first term can be estimated using the strategy of Lutsko and Tóth. Due to the restriction $\xi\leqslant 10$ we do not obtain a logarithmic correction:

$$\lambda\left((u,\xi,v)\in\tilde{A}:\tau>s,\xi\leqslant 10\right)\leqslant\frac{C}{1+s}.$$

The other term we split further into

$$\lambda\left((u,\xi,v)\in\tilde{A}:\tau>s,\xi\geqslant 10\right)=\lambda\left((u,\xi,v)\in\tilde{A}:\tau>s,\xi\geqslant 10,N=3\right)$$
$$+\sum_{k=4}^{\infty}\lambda\left((u,\xi,v)\in\tilde{A}:\tau>s,\xi\geqslant 10,N=k\right).$$

We now turn to the proof of (2.15). Under the constraints $N=3$ and $\xi\geqslant 10$, we know that $\tau\leqslant 3\xi$, and therefore

$$\lambda\left((u,\xi,v)\in\tilde{A}:\tau>s,\xi\geqslant 10,N=3\right)\leqslant\int_{s/3}^{\infty}P\left(\angle(u,v)\leqslant(1+\xi)^{-1}\right)\leqslant\frac{C}{1+s}.$$

Finally, the estimate (2.16) for the contribution of higher number of collisions can be bounded using the iterated form of (2.6). We first observe that

$$n_{\ell}\geqslant\tfrac{1}{2}\left(\tfrac{\xi}{2}\right)^{\ell-2}|e\cdot(u\times v)|. \tag{2.26}$$

We have $\tau\leqslant 2N\xi$ and N collisions require

$$n_{N-1}\xi\leqslant 1.$$

Combining these estimates we obtain

$$\lambda\left((u,\xi,v)\in\tilde{A}:\tau>s,\xi\geqslant 10,N=k\right)$$
$$\leqslant\int_{s/(2k)\wedge 10}^{\infty}\int_{\mathbb{S}^2}\int_0^{1/\xi}\mathbb{1}\left(\tfrac{1}{2}\left(\tfrac{\xi}{2}\right)^{k-3}\xi|e\cdot W|\leqslant 1/t\right)t\,dt\,dS(W)\,d\xi$$
$$\leqslant C\int_{s/(2k)\wedge 10}^{\infty}\int_0^{1/\xi}\frac{2^k}{\xi^{k-2}}\,dt\,d\xi\leqslant C\int_{s/(2k)\wedge 10}^{\infty}\frac{2^k}{\xi^{k-1}}\,d\xi\leqslant\frac{C^k}{s^{k-2}},$$

where we use $k\geqslant 4$. Summing over $k\geqslant 4$ yields, for $s\geqslant 2C$ large enough

$$\lambda\left((u,\xi,v)\in\tilde{A}:\tau>s,\xi\geqslant 10,N\geqslant 4\right)\leqslant\frac{2C^2}{s^2}.$$

Since we know the value is bounded for $0\leqslant s\leqslant C$, this finishes the proof. $\qquad\square$

2.3. Exit distribution of simple direct recollisions

The estimates in lemma 2.4 identify the probability of recollision events with $N=3$, i.e. only one back-scattering, as having non-integrable decay in $s\geqslant 1$. Hence, these events are one of the obstacles for the future goal of reaching timescales with $\lim_{r\to 0}T(t)r^2=0$, which will requires to avoid any logarithmic divergences. Since we believe the estimates to be sharp, we would like to examine the geometry of these collision events closer and give an idea how this problem could be overcome in the future. More precisely, we will show that the direct recollision events with very long flight times that are responsible for the logarithmic divergence essentially recouple to the free flight process, because we can prove that the exit velocity of the tagged particle becomes uniformly distributed and independent of the entry velocity as $\xi\to\infty$.

With the notation of the last section, we recall that the exit distribution for $N=3$, is given by

$$\tilde{w}=v-2(v\cdot\omega)\omega, \tag{2.27}$$

where $\omega=\frac{Z(\tau_2)-a}{|Z(\tau_2)-a|}\in\mathbb{S}^2$ is the direction of the transfer of momentum.

Lemma 2.7. *We have the following convergence for the conditional exit distribution in total variation norm:*

$$\sup_{A \subset \mathbb{S}^2} \left| P(\tilde{\omega} \in A | \xi = R, u = \nu, N = 3) - \frac{|A|}{|\mathbb{S}^2|} \right| \leqslant \frac{C}{1+R}. \tag{2.28}$$

Proof. Let $\xi = R$ and $u \in \mathbb{S}^2$ be arbitrary, and $N = 3$. Then the exit velocity $\tilde{w}$ is given by (2.27), where ω is a function of u, ν and ξ. We compute the conditional probability density as

$$\rho_{\xi=R, u=\nu}(\tilde{w}) = \frac{1}{\mathcal{Z}} \left(1 + 2d\cos\alpha\right)^{-1} \left(1 + 2d/\cos(\beta)\right)^{-1} \mathbb{1}_{\cos\alpha > 0},$$

where $d = |Z(\tau_2) - Z(\tau_1)|$ is the distance between the last two collisions, α is the angle between $-\nu$ and ω, and $\beta = \angle(\omega, Z(\tau_1) - a)$. Moreover, $\mathcal{Z}$ is the surface volume

$$\mathcal{Z} = \int_{\mathbb{S}^2} \mathbb{1}_{N(\nu, u, \xi) = 3} \, d\nu,$$

where $N(\nu, u, \xi)$ is the number of collisions in the event as a function of the parameters. From this we obtain

$$\left| \rho_{\xi=R, u=\nu}(\tilde{w}) - \frac{1}{\mathcal{Z}} \frac{1}{4R^2} \right| \leqslant \frac{C}{1+R}, \quad \text{for } \tilde{w} \in \text{supp } \rho_{\xi=R, u=\nu}.$$

Since $\mathcal{Z}$ satisfies

$$\mathcal{Z} = \frac{\pi}{R^2} + O\left(\frac{1}{R^3}\right),$$

we obtain

$$\left| \rho_{\xi=R, u=\nu}(\tilde{w}) - \frac{1}{4\pi} \right| \leqslant \frac{C}{1+R}, \quad \text{for } \tilde{w} \in \text{supp } \rho_{\xi=R, u=\nu}.$$

The convergence of the conditional density to the uniform density shows that

$$\text{Uni}\left(\mathbb{S}^2\right) \left(\{\tilde{w} \notin \text{supp } \rho_{\xi=R, u=\nu}\}\right) \leqslant \frac{C}{1+R}$$

as well, and the claim follows. $\square$

As discussed in the introduction, these events are not the only ones yielding error terms that become significant on timescales $T(t) \sim r^{-2}|\log r|^{-1}$. In particular some of these terms are generated by two subsequent scattering events, which could only be treated by considering a different auxiliary process with longer memory. For the moment, we only state these additional estimates on direct recollisions for application in future research.

3. Application to the invariance principle of Lutsko and Toth

We show how the improved geometric estimates give the following improved validity of the invariance principle in [13]. We use the notation X^r for the empirical Random Lorentz gas, Y for the Markovian free flight process and W for the standard Wiener process of variance 1 in $\mathbb{R}^3$.

Theorem 3.1. *Let $T = T(r)$ be such that $\lim_{r \to 0} T(r) = \infty$ and $\lim_{r \to 0} r^2|\log r| T(r) = 0$. Then, for any $\delta > 0$,*

$$\lim_{r \to 0} \mathbf{P}\left(\sup_{0 \leqslant t \leqslant T} |X^r(t) - Y(t)| > \delta\sqrt{T} \right) = 0 \tag{3.1}$$

and hence

$$\left\{ t \mapsto T^{-1/2} X^r(Tt) \right\} \Rightarrow \{ t \mapsto W(t) \} \tag{3.2}$$

as $r \to 0$ in the averaged-quenched sense.

The proof of the corresponding result in [13] is the core part of their paper. A key ingredient is the construction of an auxiliary Z-process via coupling with the same data which ignores interaction beyond direct shadowing and direct recollisions with the last seen scatterer. The difference between the Lorentz exploration process and the Z process is estimated in [13, proposition 1] using various geometric estimates. Our improved geometric estimates above yield improved estimates for the auxiliary process:

Proposition 3.2. *There exists $C < \infty$ such that for arbitrary incoming and outgoing velocities*

$$\mathbf{P}\left(\mathcal{X}(t) \not\equiv Z(t) : 0^- < t < \theta^+\right) \leqslant Cr^2|\log r|. \tag{3.3}$$

This improved proposition is enough to obtain the longer time scales:

Proof of theorem 3.1. Using the same arguments as in [13], proposition 3.2 allows an improvement of the stopping time estimates [13, lemma 9] to a timescale $\lim_{r\to 0} T(r) = \infty$ and $\lim_{r\to 0} r^2|\log r|T(r) = 0$. The other main ingredient [13, lemma 10] holds already on longer timescales. Both lemmas together yield (3.1), which then implies (3.2) due to the invariance principle of the Markovian flight process. $\qquad\square$

Remark 3.3. The inequality (3.3) is sharp in the sense that mismatches between the two processes do occur with probability $\sim r^2|\log(r)|$. To see this, consider two consecutive free flights $Y_i = \xi_i\omega_i$ $(i = 1, 2)$ given by independent random variables $\xi_i \sim \mathrm{Exp}(1)$, $\omega_i \sim \mathrm{Uni}(\mathbb{S}^2)$. Then the probability of entering an r neighbourhood of the origin after the two flights satisfies:

$$P(|Y_1 + Y_2| \leqslant r) \geqslant cr^2|\log r|.$$

This means mechanical inconsistencies appear due to *indirect* recollisions with this frequency, which cannot be taken into account by the auxiliary process Z. See also [13, remarks on dimension (3)].

It remains to show proposition 3.2. The key challenge is to improve [13, (66)], which deals with the case that there is exactly one k with direct shadowing ($\hat{\eta}_j = 1$) or a direct recollision with the directly previous scatterer ($\tilde{\eta}_k = 1$) but not both. All other cases have already been estimated to be of higher order in [13]:

Lemma 3.4. *Suppose that the Lorentz exploration process and the auxiliary process are constructed as in [13] on different intervals indexed with $j = 1, \ldots, \gamma$ for $\gamma \in \mathbb{N}$. Furthermore, assume*

$$\mathbf{P}\left(\left\{\mathcal{X}(t) \not\equiv Z(t) : 0^- < t < \theta^+\right\} \cap \left\{\sum_{j=1}^{\gamma} \eta_j = 1,\right\}\right) \leqslant Cr^2|\log r|, \tag{3.4}$$

then proposition 3.2 holds.

Proof. The proof of the corresponding proposition in [13] is based on bounds [13, (64),(65),(66)] for the cases that $\sum_{j=1}^{\gamma} \eta_j$ is > 1, $= 0$ and $= 1$ respectively. The first two cases have already bounds consistent with proposition 3.2. The new bound in (3.4) then yields the improved proposition 3.2. $\qquad\square$

Next, we outline the necessary changes to obtain (3.4) and reduce the order to $r^2|\log r|$. As a first step, we improve the estimates (82) and (83) in [13, corollary 2].

Lemma 3.5. *There exist a constant $C < \infty$ such that*

$$\mathbf{P}\left(\{\hat{\eta}_k = 0\} \cap \{\tilde{\eta}_k = 1\} \cap \left\{\min_{\tau_{k-2} \leqslant t \leqslant \tau_k} \left|Z^{(k)}(t) - Z^{(k)}(\tau_{k-3})\right| < s\right\}\right)$$
$$\leqslant Cr\max(s, r|\log r|), \tag{3.5}$$

$$\mathbf{P}\left(\{\hat{\eta}_k = 0\} \cap \{\tilde{\eta}_k = 1\} \cap \left\{\min_{\tau_{k-3} \leqslant t \leqslant \tau_{k-1}+\tilde{\beta}} \left|Z^{(k)}(t) - Z^{(k)}(\tau_{k-3})\right| < s\right\}\right)$$
$$\leqslant Cr\max(s|\log s|, r|\log r|). \tag{3.6}$$

Proof. We outline the steps that need to be changed. For (3.5), we need to consider [13, (104)], where the main term to estimate is:

$$\int_{\tilde{A}_r} \min\left(\frac{s}{\angle(-e, \tilde{w})}, 1\right) \mathrm{d}\mu(u, h, v)$$
$$\leqslant \int_{\tilde{A}_r, \angle(-e, \tilde{w}) \leqslant s} \mathrm{d}\mu(u, h, v) + \int_s^\pi \int_{\tilde{A}_r, \angle(-e, \tilde{w}) = x} \frac{s}{x} \mathrm{d}\mu(u, h, v)\, \mathrm{d}x$$
$$\leqslant Crs + \int_s^\pi \int_{\tilde{A}_r, \angle(-e, \tilde{w}) \leqslant x} \frac{s}{x} \mathrm{d}\mu(u, h, v)\, \mathrm{d}x \leqslant Crs + Csr \int_s^\pi \frac{1}{1 + \frac{1}{x}} \frac{1}{x} \mathrm{d}x$$
$$= Crs + Csr\left[\log(1 + \pi) - \log(1 + s)\right] \leqslant Crs, \tag{3.7}$$

where we used (2.17), (2.18) and (2.19) to estimate the angles. All other estimates to prove [13, corollary 2, (82)] are unchanged.

For (3.6), we need to adapt [13, (107)], where the term yielding squared logarithmic corrections involves the trapping time β using (2.20) and (2.21). After scaling with r we are integrating over the collision time parameterised by x, the volume of the outgoing velocities can be bounded by $\frac{1}{1+(x/r)^2}$, then we obtain

$$
\begin{aligned}
\mathbf{P}(\{\hat{\eta}_k = 0\} &\cap \{\tilde{\eta}_k = 1\} \cap \{\xi_k < 4\beta\}) \\
&\leqslant C \int_0^\infty \frac{r}{1+x} \exp(-x) \frac{1}{1+(x/r)^2} \, \mathrm{d}x \\
&\leqslant C \int_0^\infty \frac{r}{1+(x/r)^2} \, \mathrm{d}x \\
&\leqslant Cr^2.
\end{aligned}
\tag{3.8}
$$

We do not change any other estimates, such that we obtain (3.6). □

It is not easily possible to improve (102) in [13], such that we cannot remove the other $|\log r|$ term in (3.5) despite obtaining better estimates here. We are now in the position to sketch how to provide the final missing estimate.

Lemma 3.6. *There exist a constant $C < \infty$ such that such that (3.4) holds.*

Proof. The improvements to [13, (82),(83)] by (3.5) and (3.6) then directly improve [13, (109)] to $C\gamma r^2 |\log r|$. The final missing ingredient are the estimates in [13, (110)], these involve Green's functions estimates as well as estimates involving (3.5) and (3.6), which directly yield improved estimates in [13, (113)], which yield estimates of order $r^2 |\log r|$ for [13, (110)] and hence for [13, (66)], i.e. (3.4) holds. □

This ensures the condition for lemma 3.4, which yields proposition 3.2, which in turn yields the invariance principle in theorem 3.1.

Data availability statement

No new data were created or analysed in this study.

ORCID iDs

Karsten Matthies ⓘ 0000-0001-8250-2538
Raphael Winter ⓘ 0000-0002-5385-4670

References

[1] Bálint P, Bruin H and Terhesiu D 2023 Periodic Lorentz gas with small scatterers *Probab. Theory Relat. Fields* **186** 159–219
[2] Bodineau T, Gallagher I and Saint-Raymond L 2015 The Brownian motion as the limit of a deterministic system of hard-spheres *Invent. Math.* **203** 493–553
[3] Bodineau T, Gallagher I, Saint-Raymond L and Simonella S 2023 Long-time correlations for a hard-sphere gas at equilibrium *Commun. Pure Appl. Math.* **76** 3852–911
[4] Bodineau T, Gallagher I, Saint-Raymond L and Simonella S 2024 Dynamics of dilute gases at equilibrium: from the atomistic description to fluctuating hydrodynamics *Ann. Henri Poincaré* **25** 213–34
[5] Bodineau T, Gallagher I, Saint-Raymond L and Simonella S 2024 Long-time derivation at equilibrium of the fluctuating Boltzmann equation *Ann. Probab.* **52** 217–95
[6] Boldrighini C, Bunimovich L A and Sinai Y G 1983 On the Boltzmann equation for the Lorentz gas *J. Stat. Phys.* **32** 477–501
[7] Caglioti E and Golse F 2010 On the Boltzmann-Grad limit for the two dimensional periodic Lorentz gas *J. Stat. Phys.* **141** 264–317
[8] Dürr D, Goldstein S and Lebowitz J L 1987 Asymptotic motion of a classical particle in a random potential in two dimensions: Landau model *Commun. Math. Phys.* **113** 209–30
[9] Fougères F 2024 On the derivation of the linear Boltzmann equation from the nonideal Rayleigh gas *J. Stat. Phys.* **191** 316
[10] Gallavotti G 1970 Rigorous theory of Boltzmann equation in the Lorentz gas *Nota interna* p 358
[11] Golse F 2022 The Boltzmann-Grad limit for the Lorentz gas with a Poisson distribution of obstacles *Kinet. Relat. Models* **15** 517–34
[12] Kesten H and Papanicolaou G C 1980/81 A limit theorem for stochastic acceleration *Commun. Math. Phys.* **78** 19–63

[13] Lutsko C and Tóth B 2020 Invariance principle for the random Lorentz gas—beyond the Boltzmann-Grad limit *Commun. Math. Phys.* **379** 589–632

[14] Lutsko C and Tóth B 2021 Invariance principle for the random wind-tree process *Ann. Henri Poincaré* **22** 3357–89

[15] Lutsko C and Toth B 2025 Diffusion of the random Lorentz process in a magnetic field *J. Math. Phys.* **66** 113302

[16] Marklof J and Strömbergsson A 2008 Kinetic transport in the two-dimensional periodic Lorentz gas *Nonlinearity* **21** 1413–22

[17] Marklof J and Strömbergsson A 2011 The Boltzmann-Grad limit of the periodic Lorentz gas *Ann. Math.* **174** 225–98

[18] Marklof J and Strömbergsson A 2024 Kinetic theory for the low-density Lorentz gas *Mem. Amer. Math. Soc.* **294** v+136

[19] Marklof J and Tóth B 2016 Superdiffusion in the periodic Lorentz gas *Commun. Math. Phys.* **347** 933–81

[20] Matthies K, Stone G and Theil F 2018 The derivation of the linear Boltzmann equation from a Rayleigh gas particle model *Kinet. Relat. Models* **11** 137–77

[21] Matthies K and Syntaka T 2024 Derivation of kinetic and diffusion equations from a hard-sphere rayleigh gas using collision trees and semigroups (arXiv:2405.04449v1) to appear in LMS lecture notes

[22] Matthies K and Syntaka T 2024 Fractional diffusion as the limit of a short range potential Rayleigh gas (arXiv:2405.19025)

[23] Nota A, Nowak D and Saffirio C 2024 Diffusion limit of the low-density magnetic Lorentz gas (arXiv:2412.11134)

[24] Nota A, Saffirio C and Simonella S 2022 Two-dimensional Lorentz process for magnetotransport: Boltzmann-Grad limit *Ann. Inst. Henri Poincaré Probab. Stat.* **58** 1228–43

[25] Nota A, Velázquez J J L and Winter R 2021 Interacting particle systems with long-range interactions: scaling limits and kinetic equations *Atti Accad. Naz. Lincei Rend. Lincei Mat. Appl.* **32** 335–77

[26] Nota A, Velázquez J J L and Winter R 2022 Interacting particle systems with long-range interactions: approximation by tagged particles in random fields *Atti Accad. Naz. Lincei Rend. Lincei Mat. Appl.* **33** 439–506

[27] Nota A, Winter R and Lods B 2019 Kinetic description of a Rayleigh gas with annihilation *J. Stat. Phys.* **176** 1434–62

[28] Sinai Y G 1970 Dynamical systems with elastic reflections. Ergodic properties of dispersing billiards *Uspehi Mat. Nauk* **25** 141–92

[29] Spohn H 1978 The Lorentz process converges to a random flight process *Commun. Math. Phys.* **60** 277–90

[30] Spohn H 1991 *Large Scale Dynamics of Interacting Particles* (*Texts and Monographs in Physics*) (Springer) (https://doi.org/10.1007/978-3-642-84371-6)

[31] Tóth B 2025 Semi-quenched invariance principle for the random Lorentz gas: beyond the Boltzmann–Grad limit *Entropy* **27** 1053

[32] Wennberg B 2023 The Lorentz gas with a nearly periodic distribution of scatterers *J. Stat. Phys.* **190** 27